

A NEW LOOK AT COPERNICAN AND ERATOSTHENIAN CRATER POPULATIONS ON THE MOON AND ASSESSMENT OF LUNAR CHRONOLOGY. L.R. Ostrach¹, N.E. Petro¹, C.I. Fassett², J.L. Whitten³, B.W. Denevi⁴, B.T. Greenhagen⁴, L.M. Carter¹, ¹NASA Goddard Space Flight Center, Greenbelt, MD, ²Mount Holyoke College, South Hadley, MA, ³Smithsonian Institution, Washington, D.C., ⁴Johns Hopkins University Applied Physics Laboratory, Laurel, MD. (contact: lillian.r.ostrach@nasa.gov)

Motivation: Identifying and characterizing young impact crater populations is critical to improve understanding of the recent geological history of the Moon, as well as the rate at which impact craters degrade and the lunar regolith evolves. Investigating impact craters from the two youngest geological epochs (the Copernican and Eratosthenian) with recently acquired lunar mission data enables re-assessment of the accepted age classification scheme for these crater populations (i.e., the “Wilhelms classification,” [1, 2]). In addition, the higher resolution and increased geographic coverage of recent datasets enables craters to be classified to smaller diameters than previously possible, thus improving local stratigraphic assessments and characterization of these young crater populations on the Moon.

Critical outstanding questions regarding the Copernican and Eratosthenian crater populations include (1) what is the global abundance of Copernican and Eratosthenian impact craters ≥ 10 km in diameter and (2) what are morphologic characteristics of young impact craters on the Moon? Answering these questions will facilitate investigations concerned with the correlation between crater age and regolith evolution, and crater age versus crater degradation state [e.g., 3]. Moreover, a global investigation of young lunar craters would enable the shape of the crater size-frequency distribution curve for the youngest crater ages to be examined in a systematic way. Remotely sensed data obtained by the Lunar Reconnaissance Orbiter (LRO), Chandrayaan-1, and Kaguya/SELENE missions provide, for the first time, an opportunity to conduct a global assessment of the two youngest age classes of impact craters on the Moon through correlation of multiple contemporary datasets.

Previous Efforts: Catalogs of lunar crater measurements date as far back as the 1800s, with a primary emphasis on crater morphometry. The most complete global assessment of the ages of lunar craters to date remains the catalog published in *The Geologic History of the Moon* [“GHM,” 1], where relative crater ages for craters ≥ 30 km in diameter were assessed on the basis of stratigraphic relations (e.g., superposition, cross-cutting) and crater morphology (e.g., degradational features) using Earth-based, Lunar Orbiter, and Apollo images. The “Wilhelms classification,” based on the original time-stratigraphic system devised by Shoemaker and Hackman [2; Fig. 1], traditionally defines Copernican- and Eratosthenian-aged craters as containing fresh, sharp crater morphologies. The primary identifier used to distinguish Copernican- from Eratos-

thenian-aged craters is the presence of ejecta rays and topographic freshness [1].

In 2009, the GHM was updated using Clementine images and additional nomenclature [4] to provide a reclassification of the ages of craters based on newer data. Since 2009, mission data have spurred numerous efforts to compile global crater catalogs [e.g., 5–12]; however, none of these efforts have re-assessed or expanded upon the original GHM catalog of crater ages.

Methods: We are currently in the process of classifying all lunar craters ≥ 10 km in diameter to identify the Copernican and Eratosthenian populations using from LRO, Chandrayaan-1 (Moon Mineralogy Mapper, M³), and Kaguya (Terrain Camera) and Clementine, as the multispectral mosaics are useful to provide a direct comparison with the most recent GHM update [4]. The updated GHM catalog [4], in addition to more recently published crater catalogs [e.g., 5–12], provided a basis for initial crater identification (e.g., latitude, longitude, diameter, accepted nomenclature) and morphology observations (e.g., presence or absence of ejecta rays, central peaks, wall terraces, etc.).

We are using LRO Wide Angle Camera and Kaguya Terrain Camera mosaics to detail crater morphology and catalog observations related to the crater interior (e.g., presence of central peak, wall terraces, impact melt ponds) and exterior (e.g., blocky ejecta, impact melt flows, presence of ejecta rays). Topographic data from LROC, LOLA, and Kaguya also are being used to analyze morphology.

Factors related to crater maturity are being examined on the basis of LRO Wide Angle Camera optical maturity [13] and Clementine optical maturity [14] data. These data assess the degree of space weathering of exposed ejecta materials and distinguish between freshly exposed ejecta rays and those that have a distinct composition compared to the surrounding terrain. Moreover, optical maturity profiles for Copernican-aged craters can be derived that may allow further relative age sub-classification [e.g., 15], thus enabling distinction of the youngest Copernican-aged craters from the remainder of the Copernican crater population.

LRO Diviner rock abundance measurements [16] provide another means to distinguish the youngest Copernican-aged craters from those that are older [e.g., 17, 18]. Measures of rock abundance in Copernican and Eratosthenian craters can thus improve relative age assessments.

M³ multispectral data [19] provide additional information to distinguish compositional ejecta rays

from those reflecting optical maturity [20]. M^3 compositional observations improve upon those made by Clementine as the wavelength coverage, in addition to higher spatial resolution, enables improved distinction between various mafic compositions.

Mini-RF measurements are used to investigate crater properties related to crater degradation. Mini-RF Circular Polarization Ratio measurements provide information about the lunar subsurface that is not readily obtained through observations of visible images (e.g., ejecta blanket properties including roughness and block abundance [21–23], and impact melt flows [24]). Additionally, observations of radar dark haloes surrounding impact craters [25] and radar properties of ejecta rays can be used to infer regolith properties.

Implications: Improving our knowledge of the chronology of impacts and the stratigraphy of the recent lunar eras is critical for interpreting the evolution of airless bodies in the Solar System. To date, no focused study to assess the Copernican and Eratosthenian crater populations has successfully defined ≥ 10 km diameter craters of these epochs in a systematic, multi-faceted way. With such a database, an improved interpretation of the last ~ 2 billion years of impacts is possible via a new size-frequency distribution for Copernican- and Eratosthenian-aged craters, as improving the understanding of the contributions to the regolith

by these craters via correlations of age and degradation state.

References: [1] Wilhelms, D.E. (1987) *USGS Prof. Paper 1348*, 302p. [2] Shoemaker, E.M., Hackman, R.J. (1962) in: *The Moon–IAU Symposium 14*, 289-300. [3] Fassett, C.I., Thomson, B. (2014) *J. Geophys. Res. Planets* 119, 2255-2271. [4] Wilhelms, D.E. Byrne, C.J. (2009) <http://www.imageagain.com/Strata/StratigraphyCraters.2.0.htm>. [5] Losiak, A., et al., (2009) *LPS 40*, abst. 1532. [6] Head, J.W., et al. (2010) *Science* 329, 1504-1507. [7] Salamunićar, G., et al. (2012) *Plan. Space Sci.* 60, 236-247. [8] Salamunićar, G., et al. (2014) *Adv. Space Res.* 53, 1783-1797. [9] Wang, J., et al. (2015) *Plan. Space Sci.* 112, 42-45. [10] Öhmann (2015) <http://www.lpi.usra.edu/lunar/surface/index.shtml>. [11] Povilaitis, R.Z., et al. (2015) *LPS 46*, abst. 2880. [12] Robbins, S. (2016) *LPS 47*, this volume. [13] Denevi, B.W., et al. (2014) *J. Geophys. Res. Planets* 119, 976-997. [14] Lucey, P.G., et al., (2000) *J. Geophys. Res.* 105, 20,377-20,386. [15] Grier, J.A., et al. (2001) *J. Geophys. Res.* 106, 32,847-32,862. [16] Bandfield, J.L., et al. (2011) *J. Geophys. Res.*, 116, E00H02. [17] Ghent, R.R., et al. (2014) *Geology* 42, 1059-1062. [18] Mazrouei, S., et al., (2015) *LPS 46*, abst. 2331. [19] Pieters, C.M., et al. (2009) *Curr. Sci.* 96, 500-505. [20] Nettles, J.W., et al., (2011) *J. Geophys. Res.* 116, E00G17. [21] Bell, S.W., et al. (2012) *J. Geophys. Res.* 117, E00H00. [22] Stickle, A.M., et al. (2015) *Icarus*, in revision. [23] Ghent, R.R., et al. (2015) *Icarus*, in press. [24] Neish, C.D., et al. (2014) *Icarus* 239, 105-117. [25] Ghent, R.R., et al. (2005) *J. Geophys. Res. Planets* 110, E02005.

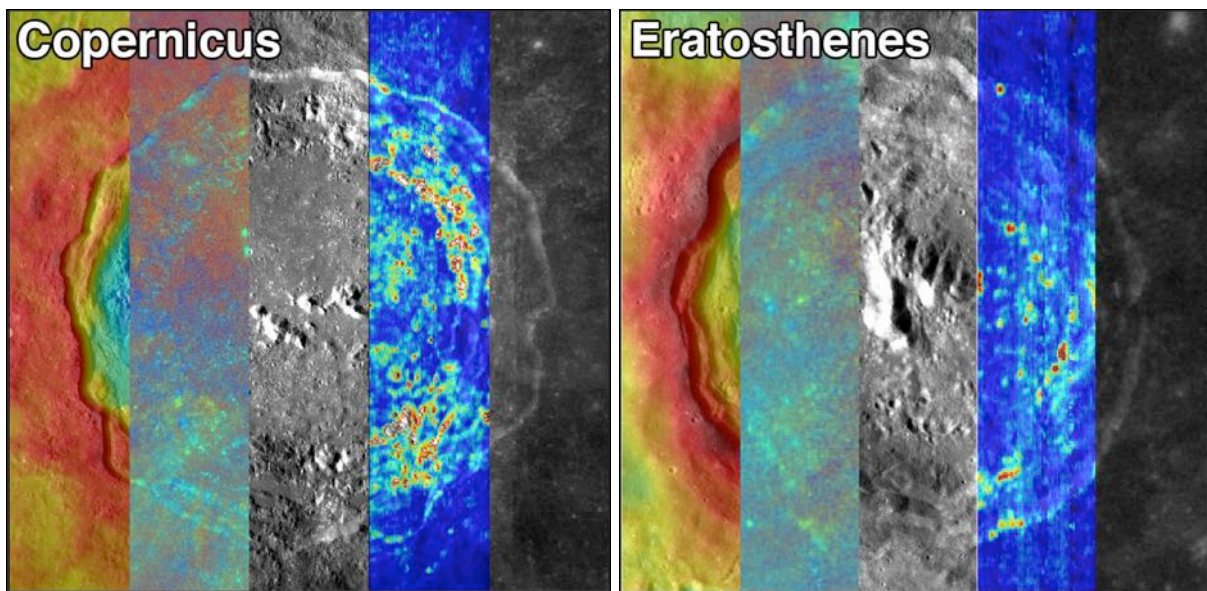


Figure 1. Lunar craters Copernicus (~ 96 km in diameter, located at 9.62°N , 339.92°E) and Eratosthenes (~ 59 km in diameter, located at 14.47°N , 348.68°E) as imaged in five datasets. From left to right, the data with qualitative, relative values are: Global lunar topography from LOLA/Kaguya (high elevation in red, lower elevation in blue), Clementine multispectral color ratio mosaic ($R=750/415$, $G=750/950$, $B=415/750$), LROC WAC global monochrome mosaic, Diviner global rock abundance (high rock abundance in red, low rock abundance in blue), and Clementine optical maturity (brighter is less mature). These datasets, among the others mentioned previously, facilitate the first integrated global assessment of Copernican- and Eratosthenian-aged craters on the Moon.